Fluorescence anisotropy sensor and its application to polymer processing and characterization

Anthony J. Bur, Steven C. Roth, and Charles L. Thomas[a)]
Polymers Division, National Institute of Standards and Technology (NIST), Gaithersburg, Maryland 20899

(Received 24 August 1999; accepted for publication 6 December 1999)

An optical sensor containing polarizing optical components has been constructed to monitor fluorescence anisotropy during polymer processing and to carry out remote sensing of polymer products doped with fluorescent dyes. The sensor is a compact unit that is used to polarize incident excitation light as well as to analyze the polarization of generated fluorescent light. Optical fibers are used to carry light between the sensor head and the light source and detecting equipment. The anisotropy measurement yields information about the orientation of a fluorescent dye molecule that has been doped into polymer matrix. Fluorescent dyes that have geometrical asymmetry in their molecular structure are used. Experiments are described for which the sensor is positioned in line during extrusion, during specimen extension, and where the sensor is used to carry out area scans of films and sheets. Measurements were made on polyethylene, polyethylene terephthalate, and polybutadiene resins that contained a low concentration of fluorescent dye.
[S0034-6748(00)04103-4]

I. INTRODUCTION

A fundamental property of polymer materials that determines their performance and properties is molecular orientation. During polymer processing, molecular orientation is caused by shear and extensional stresses applied to the material. Optical methods that can be used to measure molecular orientation are birefringence,[1–3] optical dichroism,[4–7] and fluorescence anisotropy.[7–17] The first two methods require that the probing light transmit through the material, but fluorescence measurements can be carried out by excitation and detection from one side only. This facilitates measurements in many circumstances involving polymer characterization and process monitoring, and is one of the motivating factors behind the development of the sensor and instrument described here.

Fluorescence anisotropy measurements yield information about both the orientation and molecular dynamics of the dye molecule.[12,18–24] The measurement has been used to measure molecular orientation in polymer melts, and in solid polymer films and fibers.[7–11,14,25] To characterize polymer systems, a dye is incorporated into the polymer matrix by mixing dye and resin at low levels of dye concentration, less than 10^{-5} mass fraction of dye in the resin. Such low concentrations do not affect the performance of the polymer product. In some cases, the polymer molecule contains fluorescent moieties that eliminate the need for adding a fluorescent dye. Also, the fluorescent dye can be covalently bonded or ''tagged'' to the polymer molecule in which case the dynamics and orientation of the dye closely mirror those of the polymer.[8,24]

Our fundamental understanding of fluorescence anisotropy and methods to measure it is primarily based on research done in the biosciences during the past 60 years. The biosciences literature is rich in both experimental and theoretical contributions which serve as a basis for the application of fluorescence measurements in polymer science.[12,26–32] Time resolved fluorescence anisotropy, phase modulated fluorescence, continuous wave fluorescence anisotropy, and continuous wave fluorescence spectroscopy are four methods used routinely in fluorescence work. The techniques yield both static and dynamic information about the molecular state and, in the case of fluorescence anisotropy, knowledge about molecular orientation is obtained. In contrast to bioscience applications, the use of fluorescent dyes to characterize polymer processing requires that the dye survive processing temperatures up to 300 °C for most polymer processing and up to 375 °C for high temperature processing. Our primary application of fluorescence has been to monitor polymer processing at operating temperatures up to 300 °C.

Measurement of fluorescence anisotropy employs excitation light polarized with respect to the laboratory coordinate system. Orientation factors are obtained from the emitted fluorescent light, which is analyzed for its polarization. Fluorescence anisotropy, r, is defined as

$$r = \frac{I_{vv} - I_{vh}}{I_{vv} + 2I_{vh}}, \tag{1}$$

where I_{vv} and I_{vh} are, respectively, vertically and horizontally polarized fluorescent light which are produced by vertically polarized excitation light. A coordinate system depicting the polarization directions is shown in Fig. 1. For polymer processing z is usually defined as the direction of resin flow and is called the machine direction of a processed sheet or film.

Orientation is defined by θ and ϕ angles of the dye absorption dipole moment where θ and ϕ are spherical coordi-

a)Present address: Department of Mechanical Engineering, University of Utah, Salt Lake City, UT 84112.

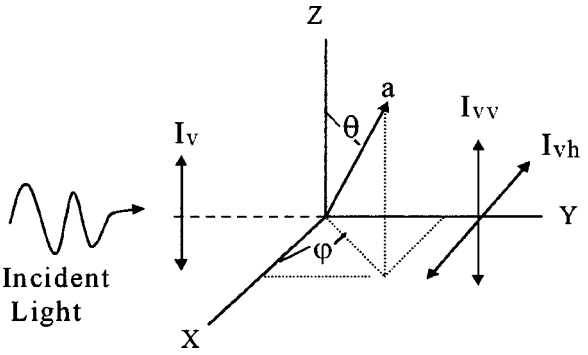

FIG. 1. Coordinate system showing polarized light orientations.

nates of the laboratory reference coordinate system of Fig. 1. Several authors have developed molecular models that yield a relationship between r and fluorescent dye orientation.[8,10,14,33,34] This relationship is somewhat complicated and involves the second and fourth moments of the cosine orientation factors. In general,

$$r = f\left(\langle \cos^2 \theta \rangle, \langle \cos^2 \phi \rangle, \frac{\tau_f}{\tau_r}\right), \tag{2}$$

where τ_f is the fluorescence decay time and τ_r is the rotational relaxation time of the molecule.[8,11,12,28] The term τ_f/τ_r appears because a molecule with small τ_r relative to τ_f will randomize its orientation before radiating fluorescence and, therefore, show no anisotropy. The ideal situation is $\tau_r \gg \tau_f$, for which the molecule is stationary while it fluoresces. Usually, $\tau_r \approx \tau_f$, for which some reorientation of the molecule occurs during fluorescence emission. Interpretation of r measurements must take into account temperature and pressure dependence of the τ_f/τ_r ratio.

In the special case of extensional flow or uniaxial extension in the z direction, the dependence on ϕ is eliminated because of axial symmetry. Fluorescence anisotropy r reduces to a less complicated expression,

$$r_{cw} = r(\infty) + [r(0) - r(\infty)]\left(\frac{\tau_f}{\tau_r} + 1\right)^{-1}, \tag{3}$$

where

$$r(0) = \frac{(2\langle P_2^2 \rangle + \langle P_2 \rangle) P_2(\cos \delta)}{2\langle P_2 \rangle + 1} \tag{4}$$

and

$$r(\infty) = \langle P_2 \rangle P_2(\cos \delta), \tag{5}$$

where P_2 is the second Legendre orientation term,

$$P_2(\cos \theta) = \frac{(3 \cos^2 \theta - 1)}{2}, \tag{6}$$

and δ is a molecular constant, the angle between the absorption and emission dipoles of the dye.[8,12] The subscript cw refers to measurements obtained using continuous wave illumination, and the brackets $\langle\ \rangle$ indicate averages over space. $r(0)$ and $r(\infty)$ are the initial and final values of anisotropy decay that would result from pulse excitation and subsequent time resolved observations. Equation (3) is for continuous illumination for which an infinite number of time resolved anisotropy decay curves are superposed.[8]

In the case of isotropic distribution of a freely rotating dye, $r(\infty) = 0$ and $r(0) = 2/5 \cos \delta (\tau_f/\tau_r + 1)^{-1}$.

For biaxially stretched film, Monnerie and co-workers have developed a model for representing anisotropy measurements in matrix form.[14] A full three-dimensional description of orientation is provided by a 3×3 matrix whose elements are the intensities of analyzed fluorescence for excitation light polarized in the x, y, and z directions. The relationship among each element of the matrix and orientation cosine factors is derived. The value of analyzed, normalized fluorescence intensity obtained for each direction is a measure of the orientation in that direction.

In order to fully understand and interpret anisotropy measurements, the values of δ and the ratio τ_f/τ_r are needed. Since δ is a constant, our main concern is the temperature and pressure dependence of τ_f/τ_r. If temperature is held constant during an experiment, it is possible to obtain a set of internally consistent data that reveal the effects of orientation. Also, if orientation is held constant while temperature changes, the change in the τ_f/τ_r ratio can be inferred. In a future publication, we will present observations of the temperature and pressure dependence of τ_f/τ_r and measurements of δ. In this article, however, we will concentrate on describing the instrumentation and evaluating sensor behavior. The data presented below were obtained at constant temperature and, with exception of the extrusion of polyethylene, pressure is also held constant.

According Eq. (1) the measurement of anisotropy involves the separate observations of I_{vv} and I_{vh}. In most commercial fluorometers, the measurement is carried out by mechanically rotating the analyzing polarizer from vertical to horizontal. If the process being observed changes faster than the time required to change the orientation of the analyzing polarizer, then useless anisotropy values are obtained. The subject of this article is the design and application of a sensor that can be used for rapid and simultaneous acquisition of I_{vv} and I_{vh} at temperatures customary for polymer processing, up to 300 °C. The sensor head can be used for remote data acquisition and operates as a one sided device thus providing access to materials and processes that are inaccessible to optical sensors requiring through transmission of light. Our primary application has been monitoring polymer processing, but the device can be used for other applications. Below, we present the results from real-time polymer process monitoring and postprocessing examination of resin products including area scans of sheets and film.

II. EXPERIMENTAL PROCEDURE

A. Fluorescence anisotropy sensor

The sensor design is shown in Fig. 2. The stainless steel sensor head has a square cross section (2.54 cm) in order to maintain a recognizable direction of the light polarization. The solid stainless steel block has been machined with channels and compartments that receive the optical fibers and optical components. Excitation light, produced by a suitable

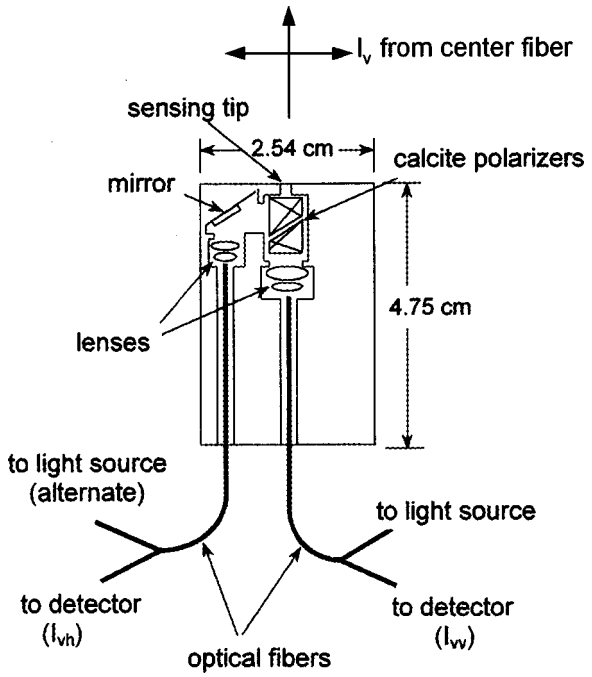

FIG. 2. Design of the square sensor head containing the polarizer, lenses, and optical fibers.

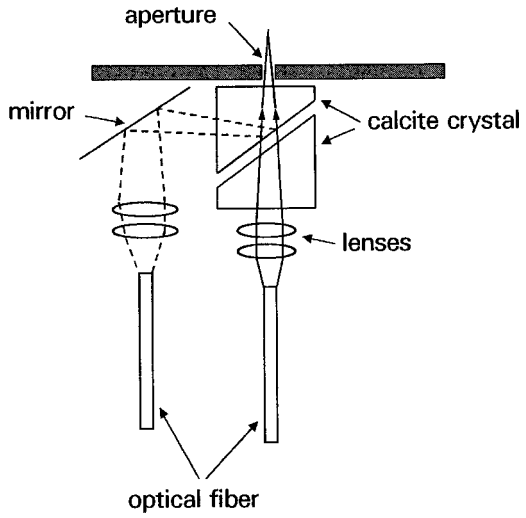

FIG. 3. Paths trasversed by light beams in the central and side channels of the sensor. Reflection from the calcite crystal to the side channel is by total internal reflection.

light source such as a laser, xenon arc lamp, or halogen lamp, is transmitted to the sensor and specimen by one of the optical fiber bundles positioned in the sensor channels. The sensor head contains a Glan–Taylor polarizer, obtained from Karl Lambrecht, consisting of two calcite crystals separated by a fixed air space of approximately 0.1 mm.[35] When assembled, the polarizer has a 6 mm sq cross section and is approximately 8 mm in length. One side surface of the calcite crystal is polished in order to allow the extraordinary ray to exit and to allow excitation light to enter from the side. Light exiting this sensor is polarized with direction parallel to a side of the square.

I_{vv} and I_{vh} are obtained simultaneously from this arrangement. Excitation light transmitted by the optical fibers in the central channel becomes vertically polarized by the calcite polarizer. The same calcite crystals analyze the polarization state of the fluorescence, i.e., it separates the fluorescence into horizontal and vertical components. The transmission paths of I_{vv} and I_{vh} through the sensor are shown in Fig. 3. The horizontally polarized fluorescence I_{vh} is internally reflected at the interface between the two polarizers, travels to the mirror, and is focused into the left channel where an optical fiber bundle collects it for transmission to the detector. The vertical component of fluorescence is transmitted straight through the calcite crystals to the optical fiber bundle in the central channel and then to the detector.

Ideally, excitation light transmitted along the central fiber bundle and through the Glan–Taylor polarizing elements traces an undeviated path. In reality, the light ray is deflected slightly to one side or the other by the birefringent crystals. To correct this, shims are used to properly position the fiber optic elements in the sensor channels so that the light beam travels through the center of the exit aperture. The shim adjustment is a small lateral shift of approximately 200 μm for our sensor, but this adjustment will be peculiar to the particular calcite crystals employed. After the correct positions are established for the fiber optic elements, set screws secure them in place.

The efficiency of the calcite crystal polarizer was examined using a helium neon laser source. The extinction ratio of the calcite polarizer/analyzer was found to be 0.05%, an error much lower than the uncertainty attributed to the photon counting statistics of our measurement. Another small error arises from reflections at crystal interfaces that permit 0.55% of the vertically polarized fluorescence to pass to the horizontal collection fibers. A correction factor is applied to the data to account for this.

The fiber optic bundles in both channels are bifurcated into two branches with one branch transmitting excitation light and the other collecting and carrying fluorescence to the detector. Both fiber cables are of identical design consisting of nineteen 200 μm core fused silica fibers, 13 of which carry fluorescence to the detector and the other 6 fibers transmit the excitation light. The fiber bundle has a specific geometrical pattern at the common end as shown in Fig. 4. One arrangement is at the top of Fig. 4: the central fiber and the 12 fibers in the outer circle are fluorescence collection fibers and go to the detector. The six fibers in the second circle carry the excitation light. Using six fibers for excitation is necessary when the light source is a xenon arc or halogen lamp because the intensity of these lamps is relatively low compared to that of a laser source. For laser excitation, we have used a fiber bundle pattern consisting of one central fiber for excitation light (bottom of Fig. 4) and the surrounding 18 fibers for fluorescence collection. At the common end (sensing tip), the fiber bundle is encased in a stainless steel tube 10 cm in length with outer diameter of 2.38 mm (3/32 in.). The total length of the fiber cable depends on the needs of the experiment. We have used 2 and 4 m fiber cable lengths with bifurcated branches having a 0.5 m length. The fiber bundle is protected over the length of the cable with stainless steel strip wound flexible sheathing. Fiber cables of

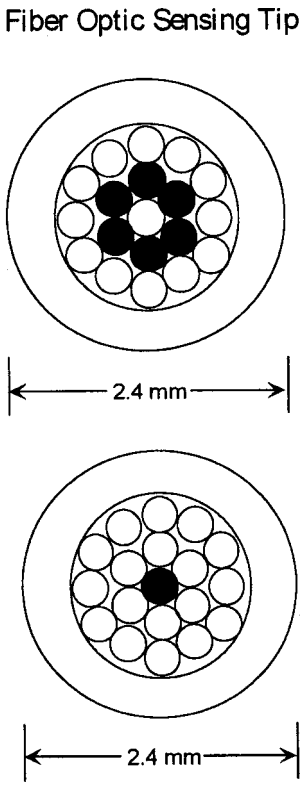

FIG. 4. Cross section of the two fiber bundle arrangements that we have used. Closed circles represent fibers carrying excitation light and open circles correspond to fluorescence collection fibers.

our custom design were purchased from Schott-CML Fiberoptics.[35]

Transmission efficiency over the two optical fiber paths is different. This requires a correction factor that is obtained by calibrating the sensor with a sample of known anisotropy. The operational expression for r becomes

$$r=\frac{I_{vv}-gI_{vh}}{I_{vv}+2gI_{vh}}, \tag{7}$$

where g is called the g-factor correction.[12] The value of g for our sensor was obtained by using a calibration standard, a solution of polydimethyl siloxane (PDMS) doped with bis (2,5-*tert*-butylphenyl) -3,4,9,10 - perylenedicarboximide (BTBP). The g factor was found to be 5.11 with a standard uncertainty of 0.04. The anisotropy of the standard solution was measured in an L-format fluorometer and found to be 0.2193 at room temperature (22.5 °C) with a standard uncertainty of 0.0016.

At the detection end, the two light signals, I_{vv} and I_{vh}, are detected by the same photomultiplier tube (PMT) (model R212 from Hamamatsu) using the chopper shown in Fig. 5 that alternately transmits the two signals to the PMT.[35] The chopper housing and drive unit were obtained from Princeton Applied Research, but the chopper blade is a custom design. The output from the PMT is a signal chopped into equally spaced bursts that is fed to the input of a two channel, gated photon counter (Stanford Research SR400).[35] By opening the gates of the two channels at the appropriate times, the two signals are separated and stored in the computer. With this arrangement, the two signals are detected by

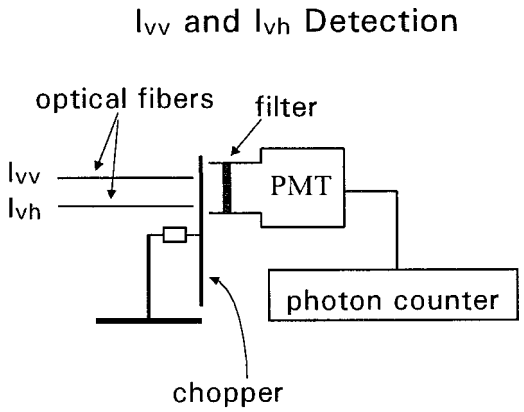

FIG. 5. Detection circuit for I_{vv} and I_{vh} using the chopper.

the same PMT and photon counter, thus avoiding problems associated with different amplification factors and drift in those factors for two detection circuits. Also, the g factor is a characteristic of the sensor alone and is independent of the PMT and photon counter amplification factors. The rate of chopper rotation is determined by the rate of change occurring in the material under investigation. For most resin processing, 50 rev/s, the rate used for the measurements presented below, is sufficiently fast.

Light transmitted to the PMT usually contains unwanted excitation light due to reflections from the lenses, the calcite crystal in the sensor head, and the specimen itself. It is possible to eliminate excitation wavelength reflections from the surface of the specimen by tilting the sensor at a small angle, but it must be noted that this will also tilt the polarization vector out of plane. Since the excitation light is at shorter wavelengths than the fluorescence, it can be minimized using cut-on and/or band pass filters positioned in front of the PMT as indicated in Fig. 5. It is difficult to eliminate entirely, however, because the reflected excitation intensity is many orders of magnitude greater than the fluorescence and attempts to eliminate it by stacking filters in series diminishes throughput of fluorescence. In some cases, the background is small compared to the fluorescence but, in general, it cannot be neglected. The initial step in carrying out an experiment is to measure the background and light source intensities. Because the background is directly proportional to the excitation light intensity, the background can be calculated from the source intensity and corrected in accordance with changes in the source intensity.

An alternative detector arrangement employed to suppress as much of the background as possible is shown in Figure 6. Here, I_{vv} and I_{vh} are detected by two PMTs, and the light is spatially filtered through a dispersing prism prior to entering the PMTs. By using the prism, excitation light at short wavelengths is deflected to a light absorbing surface at the side of the PMT aperture, and the fluorescence is directed through the aperture. Interference filters are also used at the entrance to the PMTs. By this technique, we have been able to eliminate 80% of the background, so that, in many cases, the background can be neglected relative to the fluorescence intensity. For this detector arrangement the g factor will be a function of the relative PMT amplification factors and the

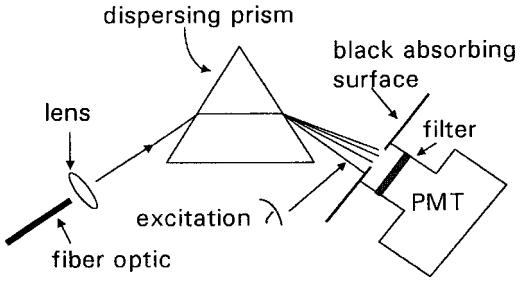

FIG. 6. Alternate detector arrangement using a dispersing prism to shunt aside the reflected excitation light.

dispersing power of the prisms, so that the entire detector package must be maintained as a single unit for a given g-factor calibration.

The sensor delivers either vertically or horizontally polarized excitation light. The optical fibers of Fig. 2 designated as the ''light source'' and ''alternate light source'' produce excitation beams with polarizations that are perpendicular to each other. Mutually perpendicular polarized excitation light beams can be produced and used to obtain anisotropy values associated with mutually perpendicular directions in the specimen, e.g., the machine and transverse directions of an extruded polymer or a stretched film. If the alternate light source is used, then I_{hh} and $I_{h\nu}$ are measured where I_{hh} is horizontally polarized fluorescence produced by horizontally polarized light and $I_{h\nu}$ is vertically polarized fluorescence produced by horizontally polarized light. Analogously, the alternate anisotropy r' is

$$r' = \frac{I_{hh} - gI_{h\nu}}{I_{hh} + 2gI_{h\nu}}. \tag{8}$$

We have used two light sources: a 75 W xenon arc lamp from Oriel Inc. and an air cooled argon ion laser from Melles Griot.[35] The xenon arc lamp has relatively low intensity but it can be used over the entire ultraviolet (UV) and visible range. The intensities of the argon ion laser lines are approximately 10^3 greater than the corresponding wavelength bands of the xenon arc lamp, but the laser can be used only for those dyes excited at the laser wavelengths.

The major source of uncertainty in the measured value of anisotropy is subtraction of the background signal. The relative standard uncertainty is estimated to be 4% when the difference $I_{\nu\nu} - I_{\nu h}$ is 10^4 counts after background subtraction, and the values of $I_{\nu\nu}$ and $I_{\nu h}$ are at least 3×10^4 counts after background subtraction. These are the lowest count levels for which reasonably precise measurements can be obtained. For some measurements reported below, obtained from experiments using a xenon arc lamp source, the relative standard uncertainty was found to be 1.5%. Higher counts yield lower uncertainty, and in the case of laser excitation, counts on the order of 10^6/s are usually observed. The relative sensitivity of the r measurement is estimated to be 0.004; this is based on our observation that, after background correction, fluorescence intensities can be measured with an uncertainty of 0.3%.

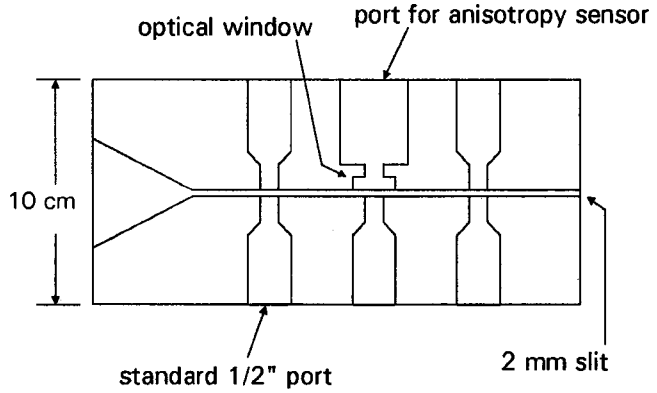

FIG. 7. Slit die rheometer containing a 2.54 cm (1 in.) sq port for the anisotropy sensor. The other ports are standard $\frac{1}{2}$ in. ports for temperature and pressure sensors.

B. Slit die rheometer

In one application, the square sensor head is inserted into a 2.54 cm (1 in.) sq instrument port in a slit die rheometer (Fig. 7). The slit die contains six instrumentation ports for pressure, temperature, and optical sensors. Implementation of the device as a rheometer requires acquisition of pressure drop, flow rate, and temperature data. During processing the slit die is attached to the exit of an extruder. Two pressure transducers are placed at the first and third positions in the slit die, separated by 50.8 mm, in order to obtain the in-line pressure drop of a flowing resin. Measurements of fluorescence anisotropy have been carried out as a function of pressure drop (shear stress) during resin extrusion through the die.

C. Extension experiments

Extension experiments were carried out using a standard materials testing machine. The sensor was mounted approximately 5 mm from the specimen as it was undergoing extensional deformation. In the case of crosslinked polybutadiene, extension was carried out in steps. At each stepwise extension, 20 min was needed to allow the specimen to relax before a reading of the anisotropy was made. The relaxation was monitored by the anisotropy and the load cell of the testing machine. For polybutadiene melt, one stepwise application of stress was applied with the resulting flow showing little recovery.

D. Area scans

Scans of anisotropy of a polyethylene terephthalate (PET) blown bottle were obtained by mounting the specimen on a translating $x-y$ stage with the sensor head placed directly above the specimen. The distance between the sensor head and specimen was less than 1 mm. All measurements were made at room temperature. Area scans were carried out by moving the sensor head in 5 mm increments between measurement positions. The scan pattern thus established was a two-dimensional 5 mm sq mesh.

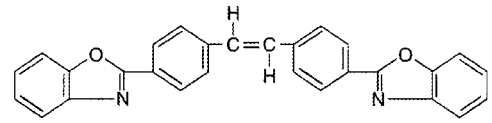

benzoxazolyl stilbene (BOS)

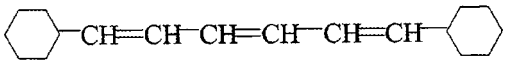

diphenyl hexatriene (DPH)

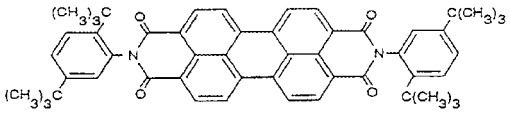

bis(-di-tert-butylphenyl)
-perylenedicarboximide
(BTBP)

FIG. 8. Molecular structures of three fluorescent dyes. For these molecules, the absorption dipole is parallel to the long axis of the molecule.

E. Materials

Three fluorescent dyes were used in this study: diphenyl hexatriene (DPH), bis(2-benzoxazolyl) stilbene (BOS), and bis (2,5-*tert*-butylphenyl) -3,4,9,10 - perylenedicarboximide (BTBP). Their molecular structures are shown in Fig. 8. For these molecules, the spectral absorption dipole that defines molecular orientation is parallel with the long axis of the molecule. All three dyes were obtained from Aldrich Chemicals.[35] We have also obtained BOS from Eastman Chemicals.[35] BOS is used in large scale commercial applications, primarily as a whitener in detergents and as an additive in food and consumer packaging, and has a blue fluorescence when excited by the mercury line at 365 nm. The excitation wavelength for DPH it is 365 nm,[12,36,37] for BOS it is 365–370 nm,[10,38,39] and for BTBP the excitation is 488 nm.[40–42] BTBP is of particular interest because it can be excited by the 488 nm line of the argon ion laser, thus imparting much higher excitation energy than would be available from the xenon arc lamp. These dyes were chosen for anisotropy studies because of their geometric anisotropy. Under applied extensional stress the long axis of the molecule is observed to orient in the direction of orientation of the matrix polymer.[8,10,14,38]

The polymers employed in our study were polybutadiene (PB), crosslinked PB (XLPB), polyethylene (PE), and polyethylene terephthalate (PET). The polybutadiene, with a relative molecular mass of 420 000, was 36% *cis*, 55% *trans*, and 9% vinyl, and was obtained from Scientific Polymer Products.[35] Crosslinked polybutadiene was prepared by irradiation with cobalt–60 gamma rays. Polyethylene (type 640 I) was obtained from Dow Chemical.[35] The polyethylene terephthalate specimen used in our experiments was obtained from a consumer product in the form of a blow molded bottle doped with BOS dye. The BOS dye was mixed with the resin in order to give the bottle the distinctive blue BOS fluorescent color. The mass fraction of BOS in the bottle product was estimated from the fluorescence intensity to be in the range of $200-300\times10^{-6}$, about an order of magnitude higher than we would normally use. The PET specimen, $55\,\text{cm}\times65\,\text{cm}\times1\,\text{mm}$ thick, was cut from the side of the bottle near the bottom at a position that was 20 cm from the top and 5 cm from the bottom.

Two methods were used to mix the dye and polymer: coating resin pellets with a solution containing the dye where the solution does not dissolve the polymer, and using a common solvent to dissolve and mix the resin and dye. For the case of polyethylene doped with BTBP, a 5 kg batch of PE pellets was prepared by pouring a solution of dye (toluene solvent) over 5% of the pellets, allowing the solvent to evaporate leaving behind BTBP coated pellets. The coated pellets were then tumble mixed with the other 95% portion of uncoated pellets so that the overall average mass fraction of dye in the polymer was 10×10^{-6}. The PE pellets were used in extrusion experiments during which additional mixing of the dye occurred during screw translation in the machine. In the case of polybutadiene, a common solvent, cyclohexane or toluene, was used to mix resin and DPH. The mass fraction of dye in the polymer was 10×10^{-6}. A sheet of DPH doped PB was obtained by spreading the solution onto a level Teflon coated polyimide sheet (contained in a circle of 15 cm in diameter), and letting the solvent slowly evaporate. Very slow solvent evaporation was achieved by placing the PB/dye solution in a desiccator with a loose fitting lid and by passing dry nitrogen very slowly (1 cm^3/min) through the desiccator. This slow evaporation process, which took several weeks to complete, resulted in a uniform, bubble free sheet of polybutadiene that had a thickness of approximately 1 mm.

The polybutadiene sheets were used in extension experiments in the neat and crosslinked conditions. Irradiation with cobalt–60 gamma rays produced crosslinked specimens with two levels of crosslink densities, $M_c=1500$ and 36 000 where M_c is the average molecular mass between crosslinks. M_c was obtained from swelling experiments using the Flory–Rehner method of solvent induced swelling in crosslinked rubbers.[43] The estimated relative standard uncertainty in the M_c measurements was 10%. These two levels of crosslinking density were chosen so that M_c was both greater than and less than the entanglement molecular mass for PB which is 2000.[44] DPH was doped into the crosslinked resin using a carrier solvent (cyclohexane) which swelled the polymer. The solvent was subsequently evaporated under vacuum and the polymer specimen was washed in order to remove any dye from the surface.

III. EXPERIMENTAL RESULTS

Data are presented from several experiments that are chosen in order to demonstrate the capability of the sensor in

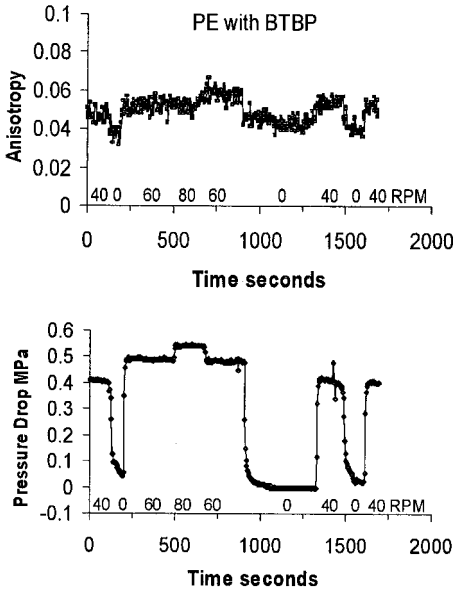

FIG. 9. Top: Anisotropy vs time for the extrusion of polyethylene doped with BTBP. The polymer was extruded through the slit die of Fig. 7. Bottom: The pressure drop between two pressure transducers separated by 5.08 cm (2 in.) plotted vs the same time scale as that for the top graph. The rpm numbers refer to the revolutions per minute of the extruder screw.

different processing situations. We show results from extension experiments on both crosslinked and neat polybutadiene, from polyethylene undergoing shear flow in the slit die rheometer, and from area scans of a polyethylene terephthalate sheet cut from a blown bottle.

In Fig. 9 anisotropy and pressure drop in the slit die versus time are plotted for extrusion of polyethylene doped with BTBP. For these data, the square sensor head was located in the slit die maintained at 160 °C; the arrangement is shown in Fig. 7. Measurements were made while increasing the extruder screw rpm from 0 to 80 and returning it to 0. The pressure drop is proportional to the shear stress applied to the flowing resin which, for this extrusion, took place at strain rates that varied from 10 to 50 s^{-1} and wall shear stress that ranged from 10^4 to 5×10^4 Pa. The anisotropy remained relatively constant as the screw rpm was increased and decreased. Small changes in the data of Fig. 9 appear to be the result of the pressure and/or temperature dependence of τ_r [Eq. (3)]. Our interpretation of these data is that the BTBP molecule is not oriented by shear stress applied to the resin during extrusion even though the sheared PE resin is flowing in the non-Newtonian shear thinning regime. We hypothesize that the dye molecule interacts with the host resin in a localized microenvironment. Shearing stresses cause orientation at macromolecular dimensions associated with intermolecular entanglements while the micromolecular neighborhoods remain relatively undisturbed. We obtained a similar result for extrusion of polyethylene and polycarbonate doped with perylene. Regarding this point, previously published anisotropy measurements carried out by the authors have shown that, if the fluorescent dye molecule is covalently bonded to the polymer molecular chain, then anisotropy becomes sensitive to shear stress because the fluorescent moiety is able to participate in the macromolecular

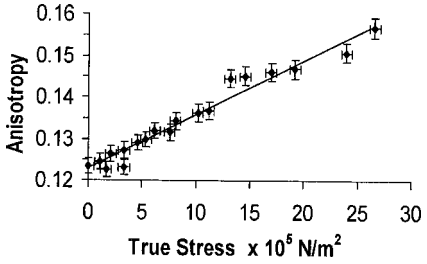

FIG. 10. Anisotropy plotted vs stress for the extension of crosslinked polybutadiene doped with DPH. The true stress is the load divided by area taking into account the change in cross sectional area as the specimen extends.

orientation of the entangled network.[8] For Fig. 9, the relative standard uncertainty in the measurements of anisotropy is 0.001, and for pressure drop the standard uncertainty is 0.02 MPa.

Although the data of Fig. 9 show that anisotropy of a free dye is insensitive to shear stresses applied during extrusion, such is not the situation for extensional stress. Resin flow during processing is often a combination of shear and extensional flows. Being able to detect the presence of extensional flow in a predominately shear flow process is a useful capability because the behavior of the final product depends on the stresses applied to it during processing. Extensional stress is of special interest to processors because it causes substantial molecular orientation relative to that caused by shear stress of the same magnitude.

We demonstrate that anisotropy of a free dye is sensitive to extensional stress in two experiments: (a) the free dye is doped into crosslinked polybutadiene and (b) the free dye is doped into the polybutadiene melt. Results of extensional experiments using crosslinked polybutadiene ($M_c=36\,000$) are shown in Fig. 10. In these experiments, the specimen behaved like rubber and achieved an extensional strain of 350% at the highest stress. We observe that anisotropy increases with applied stress and has a linear dependence on stress. The slight deviation from the straight line fit to the data at stress $\approx12\times10^5$ N/m^2 was due to the onset of strain induced crystallization in the specimen. It is interesting to note that, even after crystallization has occurred, the nearly linear relationship between anisotropy and stress is maintained. Increasing anisotropy with applied stress means that the DPH absorption dipole, or the long axis of the molecule, orients in the direction of extension. Also, in contrast to the results of the shear experiments, the data indicate that extensional stress imparts orientation to the resin at the micromolecular level. The standard uncertainties in the anisotropy and stress measurements are 1.5% for anisotropy and 0.5×10^5 N/m^2 for stress.

The extension of the polybutadiene melt was carried out by placing a strip of the resin in a mechanical testing machine and extending it at a rate of 0.833 cm/s. Anisotropy data were acquired every 100 ms during extension. The anisotropy measurements versus time are shown in Fig. 11. From time=0–2 s, no stress was applied to the specimen. At $t=2$ s, a step function stress was applied and the polymer flowed at a strain rate of 0.098 s^{-1}. For $t>2$ s, anisotropy was constant, indicating that a flow balance between the ap-

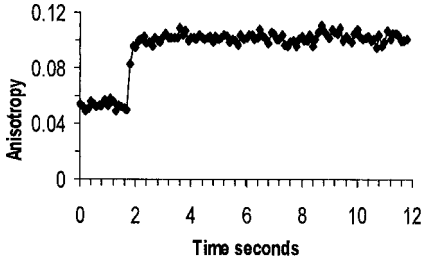

FIG. 11. Fluorescence anisotropy plotted vs time for polybutadiene melt doped with DPH. Extensional stress was applied at $t=2$ s.

plied stress and the viscous/elastic force of the material had been achieved. As with the crosslinked specimen, increasing anisotropy is interpreted as orientation of the long axis of the DPH molecule in the direction of flow. The standard uncertainty of the anisotropy data in Fig. 11 is 0.002.

Figure 12 is a contour plot of anisotropy measurements on a BOS doped PET specimen cut from the side of a blow molded bottle. The contour data are for excitation light polarized in the *y* direction, i.e., the vertical axis of the contour plot. (The increasing *y* direction points from the bottom to the top of the bottle.) The data show gradual shifts in anisotropy over the scanned area and show the presence of anisotropy or stress gradients. Also, anisotropy increases with increasing *y* showing the trend in extensional orientation as the bottle was blown. The relative standard uncertainty in the data of Fig. 12 is 1.5%. PET doped with BOS has been the subject of other studies in the literature.[10,14,38] Nobbs and co-workers demonstrated that the long axis orientation of BOS is nearly the same as the average orientation of the PET matrix. They also showed that orientation measurements made by birefringence, x-ray, and fluorescence anisotropy were in essential agreement. Lappersonne and co-workers showed how I_{vv} and I_{hh} can be used to describe orientation in biaxially oriented films of PET.

The data of Figs. 9–12 demonstrate the application of the NIST anisotropy sensor as both a real-time process monitoring tool and as a materials characterization tool. Its main advantages are that it can be used as a remote sensor to access various locations in a process line and it can be used at polymer processing temperatures. Future publications will concentrate on the interpretation of anisotropy measurements in terms of orientation factors and materials properties and include the effects of τ_r and cos δ.

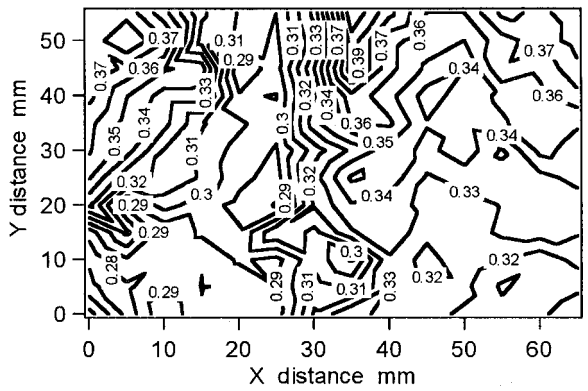

FIG. 12. Contour plot for an anisotropy area scan of a PET sheet doped with BOS. The sheet was cut from the side of a blown bottle.

[1] G. R. Cantrell, C. C. McDowell, B. D. Freeman, and C. Noel, J. Polym. Sci., Part B: Polym. Phys. **37**, 505 (1999).
[2] S. Osaki and M. Mori, Rev. Sci. Instrum. **70**, 1794 (1999).
[3] M. Okamoto, H. Kubo, and T. Kotaka, Polymer **39**, 3135 (1998).
[4] N. J. Everall, Appl. Spectrosc. **52**, 1498 (1998).
[5] T. Itadani and K. Saito, Mater. Chem. Phys. **54**, 194 (1998).
[6] J. Sakata, Thin Solid Films **333**, 213 (1998).
[7] Y. Nishio, H. Suzuki, and K. Sato, Polymer **35**, 1452 (1994).
[8] A. J. Bur, C. L. Thomas, S. C. Roth, and F. W. Wang, Macromolecules **25**, 3503 (1992).
[9] B. Erman and L. Monnerie, Polymer **28**, 727 (1987).
[10] J. H. Nobbs, D. I. Bower, I. M. Ward, and D. Patterson, Polymer **15**, 287 (1974).
[11] L. L. Chappoy, K. Rasmussen, and D. B. DuPre, Macromolecules **20**, 680 (1979).
[12] J. R. Lakowicz, *Principles of Fluorescence Spectroscopy* (Plenum, New York, 1983).
[13] J. Matsui, M. Mitsuishi, and T. Miyashita, Macromolecules **32**, 381 (1999).
[14] P. Lappersonne, P. Sergot, L. Monnerie, and G. LeBourvellec, Polymer **30**, 1558 (1989).
[15] M. L. Skytt, J. F. Jansson, and U. W. Gedde, Polym. Eng. Sci. **38**, 1270 (1998).
[16] U. A. Vanderheide, B. Orbons, H. C. Gerritsen, and Y. K. Levine, Eur. Biophys. J. Biophys. Lett. **21**, 263 (1992).
[17] J. L. Viovy and L. Monnerie, Adv. Polym. Sci. **67**, 99 (1985).
[18] L. Monnerie, Makromol. Chem., Macromol. Symp. **48–9**, 125 (1991).
[19] G. A. Baker, A. N. Watkins, S. Pandey, and F. V. Bright, Analyst (Cambridge, U.K.) **124**, 373 (1999).
[20] T. A. Smith, M. Irwanto, D. J. Haines, K. P. Ghiggino, and D. P. Millar, Colloid Polym. Sci. **276**, 1032 (1998).
[21] D. Vyprachticky, V. Pokorna, J. Pecka, and F. Mikes, Macromolecules **30**, 7821 (1997).
[22] B. M. Conger, J. C. Mastrangelo, and S. H. Chen, Macromolecules **30**, 4049 (1997).
[23] H. Aoki, J. Horinaka, S. Ito, and M. Yamamoto, Polym. Bull. **39**, 109 (1997).
[24] J. L. Viovy, L. Monnerie, and F. Merola, Macromolecules **18**, 1130 (1985).
[25] S. Maruse, M. Hirami, Y. Nishioi, and M. Yamamoto, Polymer **38**, 4577 (1997).
[26] G. Weber, J. Chem. Phys. **66**, 4081 (1977).
[27] G. Weber, Biochem. J. **51**, 145 (1952).
[28] G. Weber, Adv. Protein Chem. **8**, 415 (1953).
[29] J. R. Lakowicz, I. Gryczynski, V. Bogdanov, and J. Kusba, J. Phys. Chem. **98**, 334 (1994).
[30] J. R. Lakowicz, B. P. Maliwal, and E. Gratton, Anal. Instrum. (N. Y.) **14**, 193 (1985).
[31] E. Gratton, Biophys. J. **57**, A28 (1990).
[32] J. M. Beechem and E. Gratton, Biophys. J. **53**, A403 (1988).
[33] A. Szabo, J. Chem. Phys. **72**, 4620 (1980).
[34] C. Zannoni, Mol. Phys. **38**, 1813 (1979).
[35] Identification of a commercial product is made only to facilitate experimental reproducibility and to describe adequately experimental procedure. In no case does it imply endorsement by NIST or imply that it is necessarily the best product for the experiment.
[36] M. Shinitzky and Y. Barenholz, J. Biol. Chem. **249**, 2652 (1974).
[37] F. G. Pendergast, R. P. Haugland, and P. J. Callahan, Biochemistry **20**, 7333 (1981).
[38] J. H. Nobbs, D. I. Bower, and I. M. Ward, Polymer **17**, 25 (1976).
[39] R. A. Badley, W. G. Martin, and H. Schneider, Biochemistry **12**, 268 (1973).
[40] W. E. Ford and P. V. Kamat, J. Phys. Chem. **91**, 6373 (1987).
[41] S. A. Eldaly, M. Okamoto, and S. Hirayama, J. Photochem. Photobiol., A **91**, 105 (1995).
[42] A. Rademaker, S. Markle, and H. Langhas, Chem. Ber. **115**, 2927 (1982).
[43] P. J. Flory and J. Rehner, J. Chem. Phys. **11**, 521 (1943).
[44] R. H. Colby, L. J. Fetters, and W. W. Graessley, Macromolecules **20**, 2226 (1987).